THE PARALLELISM BETWEEN THE ACTION POTENTIAL, ACTION CURRENT, AND MEMBRANE RESISTANCE AT A NODE OF RANVIER

By I. TASAKI AND W. H. FREYGANG, JR.

(From the National Institutes of Mental Health and Neurological Diseases and Blindness of the National Institutes of Health, Public Health Service, Department of Health, Education, and Welfare, Bethesda)

(Received for publication, May 2, 1955)

The electrical activity of neural tissue is associated with changes in ionic permeability occurring at the membrane. In accord with this view, Cole and Curtis (1) and Grundfest *et al.* (2) have demonstrated a marked decrease in the membrane resistance of the squid giant axon during activity. Similar changes in the nodal membrane impedance of a frog nerve fiber have been observed by Tasaki and Mizuguchi (8, 11). The records of Cole and Curtis (1) show that the duration of the membrane resistance change outlasts the action potential in the squid giant axon.

This report describes the simultaneous recording of the action potential and membrane resistance and of the action current and change in impedance during activity at a single node of Ranvier of an isolated frog or toad nerve fiber. When the activity was limited to a single node by depriving the neighboring nodes of their excitability, a close parallelism was found between the action potential, action current, and resistance. The implications of the parallelism found in this study are discussed in relation to the theory of electrical activity postulated for the squid giant axon by Hodgkin and Huxley (4).

Method

The arrangement of apparatus illustrated in Fig. 1 A was employed for recording simultaneously the action potential and the action current of a node of Ranvier. The single nerve fiber of 12 to 15 μ outside diameter that was selected from the sciatic nerve of the frog (*Rana catesbiana*) or toad (*Bufo marinus*) had a node in the middle of the 3 mm. dissected portion. The node to be studied, N_1, was placed in the center of the middle pool of Ringer which was 1 mm. wide. The nerve end containing node N_2 was placed on the grid electrode and in isoosmotic KCl or 0.1 per cent cocaine-Ringer to inactivate it. The undissected nerve containing node N_0 was in the pool of approximately 0.1 per cent cocaine-Ringer that maintained N_0 inactive also. The portions of the nerve fiber exposed to air between the pools were approximately 0.5 mm. long. All electrodes were Ag–AgCl wires in Ringer-agar that had equal potentials when in Ringer.

Square voltage pulses for direct stimulation and resistance measurement of N_1 were applied across the 100 ohm resistor. The voltage produced by action currents

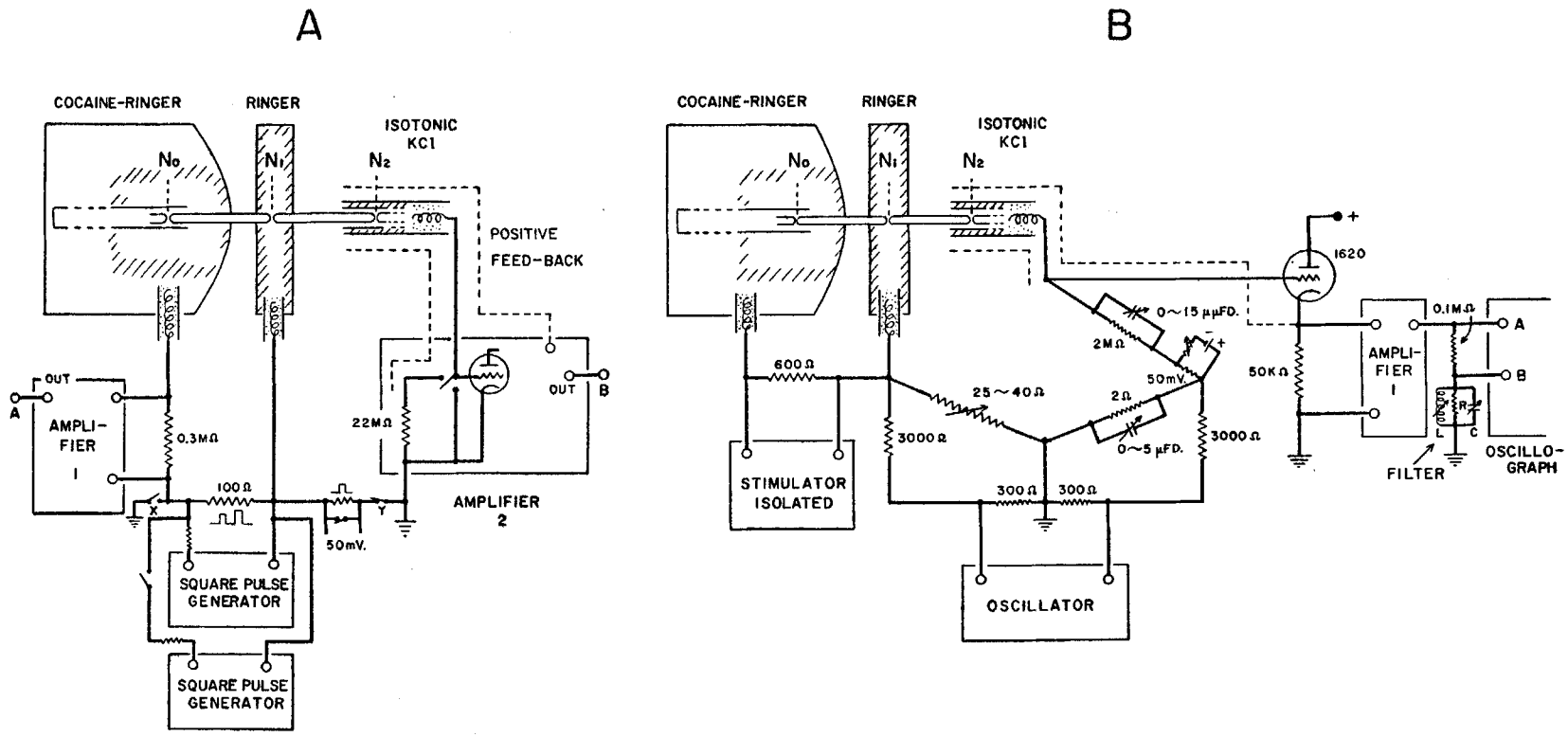

FIG. 1. Diagram illustrating methods used for the simultaneous measurement of action potential and current or action current and resistance (A), and action current and impedance (B). L = 1 henry, resistance of coil = 100 ohms, C = 0.002 μfd., R = 0.1 megohm.

passing through the 0.3 megohm resistor was amplified differentially with a Tektronix type 122 pre-amplifier (amplifier 1). Usually switch X was open and switch Y was closed as shown in Fig. 1. Alternatively, switch X was closed and switch Y opened to minimize the shock artifact introduced into amplifier 1.

The input to the grid electrode of the first stage of amplifier 2 should register the potential difference across the membrane of N_1 because of the high resistance from the pool of N_2 to ground (10). This potential difference was attenuated by 20 to 40 per cent under the usual recording conditions but could be measured more accurately after increasing the external resistance between N_2 and ground by allowing the Ringer on the fiber to dry. An input resistance of approximately 10^{10} ohms to direct current was obtained with amplifier 2 which was designed by MacNichol and Wagner (6). The shield of the grid electrode extended almost to the electrode tip and was driven by the output of amplifier 2 in order to obtain positive feed-back to the grid lead. The positive feed-back was adjusted to produce a $1/e$ rise in output voltage within 30 μ sec. after the 50 mv. voltage step was introduced between N_1 and N_2. A 22 megohm resistor could be attached to the input of amplifier 2 and the resistance between N_2 and ground was calculated from the attenuation of the signal. The grid was grounded to determine the D.C. base line. The outputs of both amplifiers were led to a Du Mont dual-beam oscillograph.

The arrangement shown in Fig. 1 B was used for the simultaneous measurement of impedance and action current. The manner of mounting and stimulating the fiber was the same as that described for Fig. 1 A, but the portion of the fiber extending from N_1 and N_2 was made an arm of a Wheatstone bridge. The voltage appearing at the grid electrode is the sum of a large potential drop caused by the action current flowing between N_2 and N_1 and a small A.C. voltage unbalance across the bridge. Channel A of the oscillograph operating at low gain displayed the amplified unfiltered signal which was essentially a record of action current, while channel B amplified the filtered A.C. signal which provided a measure of the impedance change at N_1. The frequency of the alternating current was between 3 and 4 kc. The time resolution is better at higher frequencies, but the bridge unbalance during activity is smaller. The amplitude of the A.C. voltage applied to the bridge was not allowed to exceed 50 mv. peak to peak since strong alternating currents are known to alter the action current (7, 12). The difference in the resting potential between N_1 and N_2 was balanced by a voltage source of approximately 50 mv. that was placed in one arm of the bridge. After the bridge had been balanced for the impedance of a resting fiber, an unbalance corresponding to a resistance change of 0.2 to 0.3 per cent was detectable.

The Ringer solution had 111.1 mM NaCl, 2.7 mM KCl, 1.8 mM $CaCl_2$, and 2.4 mM $NaHCO_3$ per liter of distilled water. Solutions of low and high potassium concentration were of the same composition as Ringer except that potassium chloride was either omitted or added in excess.

Experiments were done between 8 to 16°C. either in a refrigerated room or a cooled chamber to lengthen the duration of the action potentials.

RESULTS

Action Potential and Current.—The traces of Fig. 2 are simultaneous recordings, made with the arrangement illustrated in Fig. 1 A, of the action current

(upper trace) flowing between N_0 and N_1 and the action potential (lower trace) developed across the membrane of N_1. These pairs of records were obtained from three different fibers. The records in each pair were taken at threshold; because of small fluctuations in excitability, there was frequently no response and only shock artifacts were recorded (upper record). The upper traces provide a measure of the current flowing in the axis-cylinder from N_1 to N_0 since the only effective return path for this current is across the terminals of amplifier 1. The recorded amplitude of the action potential is slightly

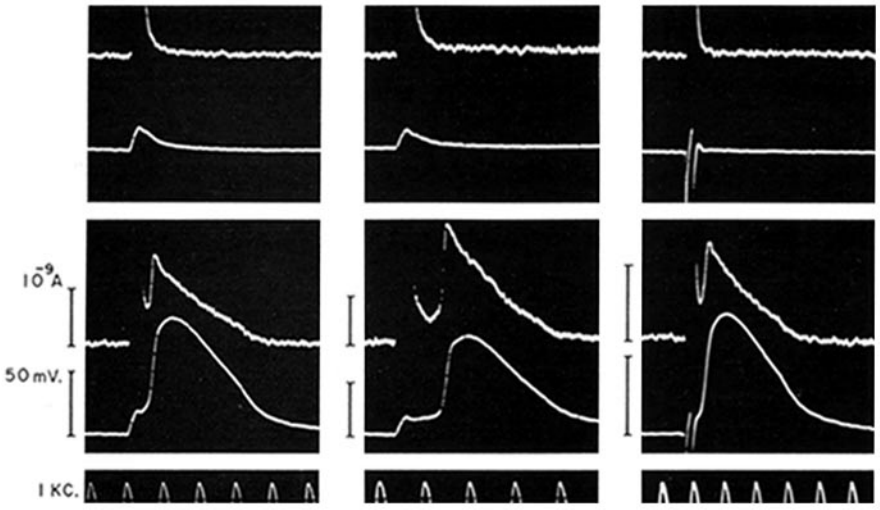

FIG. 2. Action current (upper trace) and action potential (lower trace) recorded simultaneously at a node. Top row, shock artifacts for threshold stimuli. The records on the right were taken with switch X in Fig. 1 A closed and Y open; the other sets were recorded with Y closed and X open. Three toad fibers at 12°C. Stimulus duration 0.5 msec. Shock artifacts for the records of current are downward and off the face of the cathode ray tube.

smaller than the change in the potential difference across the membrane of N_1 because of the small flow of current between N_1 and N_2 (see Method).

The time courses of action current and potential are similar except that the current reaches its peak before the voltage does. Such a deviation from parallelism should be produced by the passive electrical properties of the cable-like fiber. In order to determine the deviation produced by these properties, a network of resistors and capacitors representing the resting state of a nerve fiber was constructed on the basis of the values obtained for the electrical constants of myelinated fibers (9). Voltage pulses shaped to approximate an action potential were applied across a "node" of the model. The resulting longi-

tudinal current flowing in the middle of the nearest "internode" of the model led the applied voltage by approximately the same time as was observed with a nerve fiber. The results obtained from the electrical analog of a fiber suggest that the faster rise of action current than of action potential is caused by the capacity between the axoplasm of the fiber and the pool containing the undissected nerve.

Action Potential and Membrane Resistance.—A measure of the resistance change across N_1 was obtained with the arrangement shown in Fig. 1 A. A

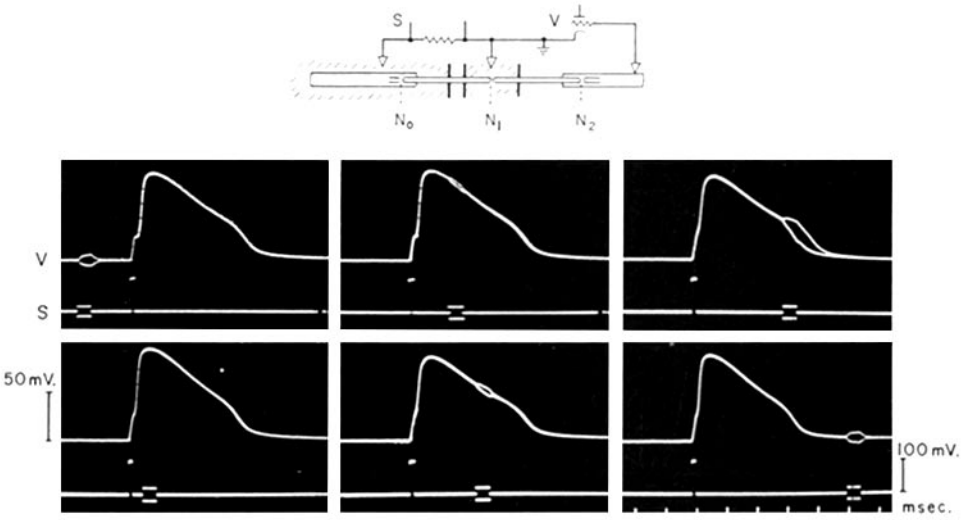

FIG. 3. Action potential and resistance recorded simultaneously at a node. *S* represents the voltage applied between N_0 and N_1. *V* is the potential difference occurring between N_1 and N_2. Two sweeps, one with a cathodal pulse and one with an anodal pulse, were superimposed in each record. The diagram is a simplification of Fig. 1 A. Toad fiber at 11°C.

pulse of either inward or outward current of 0.25 to 0.5 msec. duration was passed through N_1 at a variable delay after the stimulating current pulse had been applied. The second current pulse passing through N_1 generated a variation in the voltage across N_1 that was recorded at N_2. The magnitude of the voltage variation appearing at N_2 was taken as a measure of the membrane resistance of N_1.

Samples of the records obtained at various times during the action potential are shown in Fig. 3. Two sweeps have been superposed for each trace shown in this figure. The upper trace (*V*) is a record of the potential difference across N_1 that shows the action potential and effect of the anodal and cathodal current pulses. The lower trace (*S*) shows the time of application of the current

pulses and the stimulus. The duration of the applied rectangular pulse was sufficient to allow the deflection to reach about 90 per cent of the final value. In the lower left record of Fig. 3 the cathodal and anodal pulses have been applied at the peak of the action potential; the resistance of N_1 is too low for their effect to be discernible.

The magnitude of the action potential and the deflection caused by the applied pulses have been normalized and plotted together in Fig. 4 to provide a comparison of the time courses of the nodal action potential and resistance.

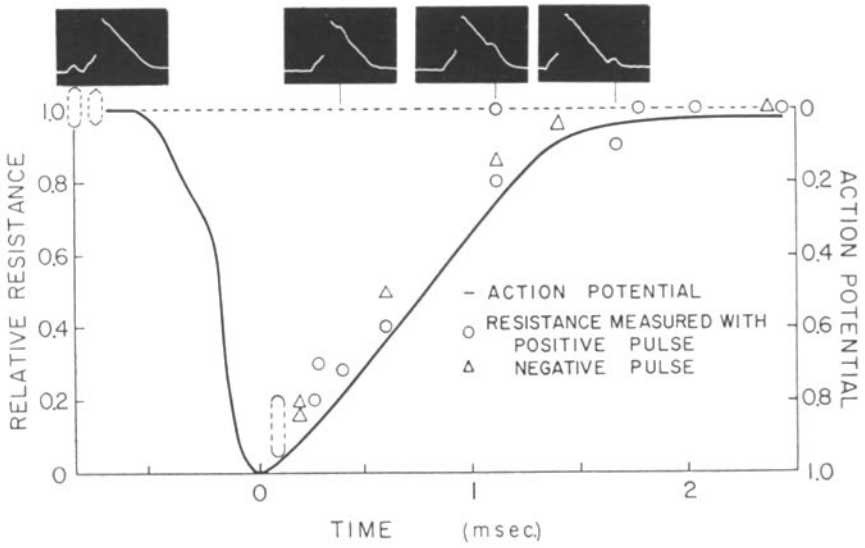

FIG. 4. Normalized action potential and resistance measurements at a node. Resistance measuring pulses applied before, during, and after the activity. Sample records are above the corresponding points. Frog fiber at 16°C.

Sample records are shown above the corresponding points. The deflection caused by the pulses (IR drop) was measured at the end of the applied rectangular pulse. The accuracy of this measurement limits the comparison but the size of the response at the peak of an action potential is less than 10 per cent of the response at the resting node.

Since the resistance of the axis-cylinder between N_0 and N_1 is of the same order of magnitude as the membrane resistance at N_1, the current generated by an applied pulse was greater during activity than at rest. Despite this complication, the magnitude of the response to the applied current pulses fell below the measurable limit during the peak of the action potential. Since the resting resistance of a node is 40 to 60 megohms (9), the nodal resistance at the peak of the action potential is less than 4 to 6 megohms.

Action Current and Membrane Impedance.—The Wheatstone bridge arrangement of Fig. 1 B was used for the simultaneous recording of the action current and the impedance change of the node N_1. The upper trace of each record in Fig. 5 shows the action current flowing in the axis-cylinder from N_1 to N_0. The lower traces in the upper row of records show the unbalance of the bridge during activity at N_1. The records in the lower row were obtained by adjusting the bridge so that it balanced during activity. The close parallelism between the time courses of the action current and impedance decrease can be observed

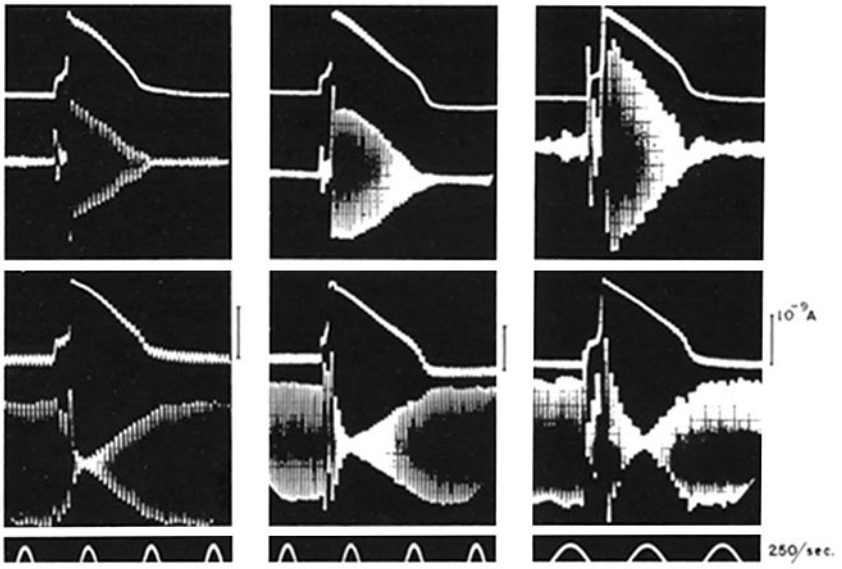

FIG. 5. Action current (upper trace) and membrane impedance (lower trace) recorded simultaneously at a node. Bridge balanced for resting impedance in upper records and for the near minimum resistance during activity in lower records. Three frog fibers at 8°C.

in this figure. Ringing of the tuned filter circuit caused by the sharp rise in action current was responsible for the irregularities at the start of the records of the impedance change. These oscillations were different in each sweep but the subsequent envelope of the alternating current was unchanged.

The maximum reduction in the measured impedance of the preparation during activity amounted to 5 to 10 per cent of the impedance at rest. This percentage is small since the resistance of the axis-cylinder between N_1 and N_2 is in series with the active membrane of N_1. The capacity of the node and the myelinated portion of the fiber in the middle pcol is approximately 3.1 $\mu\mu$fd.(9). The resistance of the nodal membrane is approximately 60 megohms

at 10°C. The resistance of the axis-cylinder between N_1 and N_2 is of the same order of magnitude. In a network consisting of a 3 $\mu\mu$fd. condenser and two 60 megohm resistors, one in parallel and the other in series with the condenser, the calculated change in the impedance of the network caused by the parallel resistance falling to zero is 8 per cent at 3.5 kc. The situation under the conditions of the experiments is complicated by the passage of alternating current through the myelin sheath, but the calculation illustrates the limited sensitivity of the method.

The voltage used for compensation of the current generated by the difference between the resting membrane potentials at N_1 and N_2 was generally 50 mv. The variation in the potential difference between normal and KCl–treated nodes observed by Tasaki and Frank (10) was between 40 and 70 mv. The compensating voltage was varied in this range. An increase in this voltage slightly increased the magnitude of the impedance loss during activity. The parallelism between the action current and the impedance loss during activity was not affected by varying the compensating voltage.

The effects of alterations in the potassium concentration of the solution surrounding N_1 were studied by the bridge method. It was found that the rate at which the membrane impedance returned to normal after the peak of the action potential could not be influenced by increasing the potassium content of the Ringer solution to 6, 9, and 12 mM/l. or by decreasing it to zero; the parallelism with the action current was unchanged.

DISCUSSION

The direction of the current flow through the node under study (N_1) was always inward during activity. The current flowing in the axis-cylinder between N_0 and N_1 is dependent upon the difference between the constant voltage across N_0 and the variable voltage across N_1. During the active depolarization of N_1 there is a flow of current through N_1 that is parallel to the voltage difference if the path is resistive. The slight deviation from parallelism shown in Fig. 2 could be predicted from the electrical constants of myelinated fibers.

The membrane action current at N_1 may be divided into its capacitative and resistive components. The resistive component of the current is associated with an ionic transfer across the nodal membrane. Tasaki (9) has estimated the capacity of the nodal membrane to be approximately 1.5 $\mu\mu$fd. The size of the action potentials measured by Tasaki and Frank (10) were about 100 mv. The falling phase of an action potential is about 10 msec. in duration at 5°C. and can be approximated by a straight line. From these data, the calculated capacitative nodal current during the falling phase of the action current is 1.5×10^{-11}A and the total charge carried by this current is 1.5×10^{-13} coulombs. Since the action current has a peak of about 2×10^{-9}A and a falling phase that may be approximated by a straight line, the total transfer of charge is about 10^{-11} coulombs at 5°C. Therefore, approximately 98 per cent of the

charge carried through the axis-cylinder between N_0 and N_1 at 5°C. is transferred by ions across the membrane of N_1.

Fig. 6 represents a modification of the equivalent circuit proposed by Hodgkin and Huxley (5) to describe the mechanism of bioelectric activity at the membrane of the squid giant axon. It is assumed that this diagram can repre-

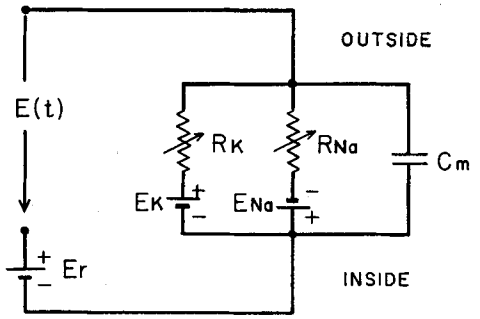

FIG. 6. Modification of the equivalent circuit proposed by Hodgkin and Huxley (5) to represent the membrane.

sent the active node of Ranvier. The batteries E_{Na} and E_K represent the equilibrium potentials for sodium and potassium ions respectively and are assumed to remain unchanged during activity. R_{Na} and R_K are the ion-specific membrane resistances which are variable and C_m is the capacity of the membrane. This capacity may be neglected since the capacitative component of the nodal current is negligible during the falling phase of the action potential. E_r represents the potential difference across the KCl-treated node (N_2) plus any voltage necessary to make the voltage $E(t)$ equal to zero during the resting state. E_p is the value of $E(t)$ at the peak of the action potential. $R(t)$ is the resistance of the network and equals R_0 when the node is inactive. The expressions $\frac{R(t)}{R_0}$ and $\frac{E_p - E(t)}{E_p}$ describe the normalized changes of membrane resistance and voltage during activity. Both expressions vary between zero and unity as in Fig. 4. R_{Na} is assumed to fall to zero at the peak of the action potential since the nodal resistance at this time is negligible compared to the resistance at rest. In Fig. 6, $R(t)$ is determined by the two parallel resistors R_{Na} and R_K:

$$\frac{R(t)}{R_0} = \frac{R_{Na} \times R_K}{R_{Na} + R_K} \times \frac{1}{R_0}. \tag{1}$$

If the total membrane current is zero in the falling phase of activity, $E(t)$ is obtained from the voltage drop across R_{Na} and the voltages of E_{Na} and E_r:

$$E(t) = (E_{Na} + E_r) - \left[\frac{E_{Na} + E_K}{R_{Na} + R_K}\right] R_{Na}. \tag{2}$$

Under the conditions of the experiment of Fig. 1 A, there is an inward current at the active node, N_1. This current, however, can be made negligibly small (or even reversed) by restoring the excitability of N_0. As will be discussed in a subsequent paper, the action potential of N_1 is practically independent of whether N_0 is normal or completely narcotized. In this simplified discussion, therefore, equation (2) is assumed to express the time course of the action potential. A more general discussion on this point is presented in the Appendix.

Since E_p is equal to $(E_{Na} + E_r)$, the expression for the normalized action potential is:

$$\frac{E_p - E(t)}{E_p} = \frac{(E_{Na} + E_K)R_{Na}}{(E_{Na} + E_r)(R_{Na} + R_K)}. \tag{3}$$

The term $\frac{(E_{Na}+E_K)}{(E_{Na}+E_r)}$ does not change with activity. The normalized expressions for resistance change (Equation 1) and action potential (Equation 3) can have parallel time courses only if R_K does not vary with activity.

In the squid giant axon, R_K is interpreted by Hodgkin and Huxley (5) as being reduced by more than 90 per cent during the falling phase of the action potential. The results of this study indicate that in the myelinated nerve fiber the potassium resistance of Fig. 6 does not change during activity by an amount greater than approximately 15 per cent; *i.e.*, within the limits of accuracy of the methods employed.

The prolongation of the impedance loss with activity observed by Grundfest *et al.* (2) in squid giant axons exposed to high external potassium concentrations was not observed at a node which was treated similarly. The cause of the prolongation is in doubt, but its occurrence can be predicted from the data of Hodgkin and Huxley (4, Fig. 14) describing the effect of depolarizations on the subsequent rate of rise of the potassium resistance. An absence of a change in potassium resistance would explain the ineffectiveness of the elevated potassium concentrations that was observed in this study. The absence of a fall in potassium resistance has been postulated by Hodgkin (3) to explain the results obtained from active Purkinje fibers of the mammalian heart by Weidmann (13).

The conclusion that the potassium resistance is constant during activity has been derived from the circuit diagram of Fig. 6. It is possible that this diagram does not apply to the node of Ranvier of the frog nerve fiber and therefore that our results do not demonstrate an unchanging permeability to potassium ions during activity.

SUMMARY

1. Simultaneous measurements of action potential and resistance and of action current and impedance change have been made at a single node of Ranvier.

2. There is a parallelism between action potential, action current, and resistance change measured at a node of Ranvier.

3. Some implications of these results have been discussed in relation to the corresponding data obtained from the squid giant axon.

REFERENCES

1. Cole, K. S., and Curtis, H. J., Electric impedance of the squid giant axon during activity, *J. Gen. Physiol.*, 1939, **22,** 649.
2. Grundfest, H., Shanes, A. M., and Freygang, W., The effect of sodium and potassium ions on the impedance change accompanying the spike in the squid giant axon, *J. Gen. Physiol.*, 1953, **37,** 25.
3. Hodgkin, A. L., The ionic basis of electrical activity in nerve and muscle, *Biol. Rev.*, 1951, **26,** 339.
4. Hodgkin, A. L., and Huxley, A. F., The components of membrane conductance in the giant axon of *Loligo*, *J. Physiol.*, 1952, **116,** 473.
5. Hodgkin, A. L., and Huxley, A. F., A quantitative description of membrane current and its application to conduction and excitation in nerve, *J. Physiol.*, 1952, **117,** 500.
6. MacNichol, E. F., Jr., and Wagner, H. G., A high-impedance input circuit suitable for electrophysiological recording from micropipette electrodes, *Naval Med. Research Inst. Research, Rep.*, 1954, **12,** 97.
7. Rosenblueth, A., Reboul, J., and Grass, A. M., The action of alternating currents upon the spike-potential magnitude, conduction velocity and polarization of nerve, *Am. J. Physiol.*, 1940, **130,** 527.
8. Tasaki, I., Nervous transmission, Springfield, Illinois, Charles C. Thomas, 1953.
9. Tasaki, I., New measurements of the capacity and the resistance of the myelin sheath and of the nodal membrane of the isolated frog nerve fiber, *Am. J. Physiol.*, 1955, **181,** 639.
10. Tasaki, I., and Frank, K., A measurement of the action potential of myelinated nerve fiber, *Am. J. Physiol.*, 1955, in press.
11. Tasaki, I., and Mizuguchi, K., The changes in the electrical impedance during activity and the effect of alkaloids and polarization upon the bioelectric processes in the myelinated nerve fiber, *Biochem. et Biophysic. Acta*, 1949, **3,** 484.
12. Tasaki, I., and Sato, M., On the relation of the strength-frequency curve in excitation by alternating current to the strength-duration and latent addition curves of the nerve fiber, *J. Gen. Physiol.*, 1951, **34,** 373.
13. Weidmann, S., Effect of current flow on the membrane potential of cardiac muscle, *J. Physiol.*, 1951, **115,** 227.

APPENDIX

A General Derivation for the Relationship between Action Potential and Nodal Resistance

Fig. 6 A is a modification of Fig. 6 in the text that allows a consideration of the current flow between N_0 and N_1.

E_K, equilibrium potential for the ionic potassium gradient across N_1.
E_{Na}, equilibrium potential for the ionic sodium gradient across N_1.
R, resistance of the axis-cylinder between N_0 and N_1 plus the resistance across N_0.
I_K, net current carried through N_1 by potassium ions.
I_{Na}, net current carried through N_1 by sodium ions.
I, net membrane current; $I = I_{Na} - I_K$.
S, voltage applied between N_0 and N_1 from a low impedance source.
V, voltage change caused by S, observed at N_2.
$E(t)$, action potential observed at N_2.
R_K^0, R_{Na}^0, and V^0; potassium resistance, sodium resistance, and voltage (V) observed at rest.
E_r, membrane voltage at rest.
E_p, peak value of action potential, $E_p = E_{Na} + E_r$.
G, G_{Na}, ...; reciprocals of R, R_{Na}, ... respectively.

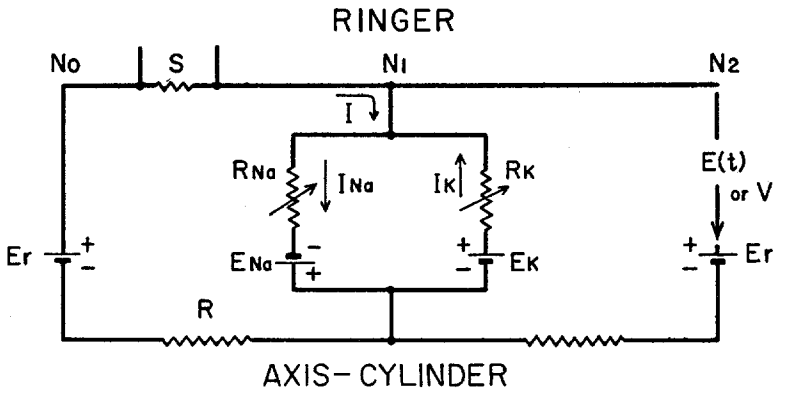

FIG. 6 A. Modification of Fig. 6 that allows a consideration of the current flow between N_0 and N_1.

Expressing the potential difference across N_1 in terms of the E.M.Fs. of the batteries and the IR drops across the resistances, the following relations are obtained:

$$E(t) - E_r = I_K R_K - E_K = -I_{Na} R_{Na} + E_{Na} = -E_r + IR.$$

Solving these simultaneous equations for I using the relation $I = I_{Na} - I_K$, we obtain

$$I = \frac{E_p R_K - (E_K - E_r) R_{Na}}{R R_{Na} + R_{Na} R_K + R_K R}, \tag{1}$$

in which the sum $(E_{Na} + E_r)$ is replaced by E_p. At rest, $I = 0$; therefore,

$$E_K - E_r = E_p R_K^0 / R_{Na}^0. \tag{2}$$

Since $E(t) = IR$, the normalized action potential is given by

$$1 - \frac{E(t)}{E_p} = \frac{R_{Na}(R_K + R + \frac{RR_K^0}{R_{Na}^0})}{RR_{Na} + R_{Na}R_K + R_KR}. \tag{3}$$

When a rectangular voltage pulse S is applied between N_0 and N_1, a potential drop (V) appears across N_1, which is given by

$$V = S \frac{\frac{R_KR_{Na}}{R_K + R_{Na}}}{R + \frac{R_KR_{Na}}{R_K + R_{Na}}}, \tag{4}$$

namely, the voltage (S) is divided into the IR drop across R and that across N_1. Using conductances instead of resistances and dividing both sides of (4) by the value of V at rest, V^0:

$$\frac{V}{V^0} = \frac{G_{Na}^0 + G_K^0 + G}{G_{Na} + G_K + G}. \tag{5}$$

Similarly, using conductances in equation (3):

$$1 - \frac{E(t)}{E_p} = \frac{\frac{G_{Na}^0}{G_K^0} \times G_K + G_K + G}{G_{Na} + G_K + G} \tag{6}$$

The results mentioned in the text indicate that, during the falling phase of action potential, the following approximate relation holds

$$1 - \frac{E(t)}{E_p} = \frac{V}{V^0}.$$

Comparing (5) with (6), it is found that they are the same when $G_K = G_K^0$, or $R_K = R_K^0$.